Available online at www.sciencedirect.com

SciVerse ScienceDirect

Procedia CIRP 8 (2013) 188 – 193

www.elsevier.com/locate/procedia

14th CIRP Conference on Modeling of Machining Operations (CIRP CMMO)

Wear Mechanism of CBN Inserts during Machining of Bimetal Aluminum-Grey Cast Iron Engine Block

Amir Malakizadi[a,]*, Ibrahim Sadik[b], Lars Nyborg[a]

[a]*Chalmers University of Technology, Department of Materials and Manufacturing Technology, SE412 96, Gothenburg, Sweden*
[b]*AB Sandvik Coromant, R&D Materials and Processes, SE126 80, Stockholm, Sweden*
* Corresponding author. Tel.: +46-31-7721-245; fax: +46-31-7721-313. *E-mail address*: amir.malakizadi@chalmers.se.

Abstract

In this study, the wear mechanism of CBN inserts while face milling of aluminum-grey cast iron engine block was investigated by means of Scanning Electron Microscopy (SEM). It was shown that the thermal cracking constitutes the main wear mechanism. The Finite Element Method (FEM) was utilized to simulate the face milling under the operational condition. The flow stress properties of the aluminum-silicon alloy and grey cast iron were determined by means of inverse methodology and the milling operation was modeled separately for each material to obtain the thermally and mechanically induced stresses on the tool edge. The methodology presented in this paper can be used to find the optimum cutting condition as well as tool geometry to reduce tool wear rate.

Keywords: Face milling; Bimetal cutting; CBN; Inverse identification.

1. Introduction

Growing demands on light weight but mechanically reliable components lead to development of bimetallic parts in car engine industry, such as bimetallic aluminum-grey cast iron engine block, in which the liner exposing to high thermal and mechanical loads is made of Grey Cast Iron (GCI), while the main body of the engine block comprises an aluminum-silicon alloy. This design concept is being practiced by different car manufacturers globally; however, there are some challenges seen in production line, such as limited tool life, severe burr formation and/or break out, poor surface roughness, etc. [1] [2].

These challenges are, in fact, attributed to use of single tool material, micro-geometry and cutting conditions for machining of two materials with different thermal and mechanical properties. Various machining concepts including coated and uncoated carbide, CBN and PCD tools are being used by industry to overcome aforementioned challenges.

In this study, several worn CBN inserts, randomly chosen from the production line, were investigated to understand the wear mechanism involved in machining of bimetal engine block under controlled cutting conditions. The main wear mode observed was due to thermal cracking. In order to understand the tool wear mechanism, the cutting process was simulated using Finite Element Method. The flow stress data of the AlSi9Cu3Fe and GCI were determined using an inverse algorithm. The temperature distribution and thermal induced stresses on the tool edge were then predicted using 3D FE modeling of the milling operation. These results can be used to find the optimum cutting conditions when machining of bimetal aluminum-grey cast iron components, which will contribute to sustainable production from both economic and environmental points of view.

2. Machining Condition and Tool Characteristics

The inserts studied in this investigation were used for finishing operation in production where the criterion for tool change is surface finish. The operational cutting condition comprises 0.1 mm feed per tooth, 0.5 mm depth of cut and cutting speed of 2300 m/min. The

doi:10.1016/j.procir.2013.06.087

effective diameter of the cutter was 315 mm and the machining process was performed under wet condition. The radial and axial rake angles were -10˚ and -6.6˚, respectively. The cutter was equipped with 11 Sandvik CB50 round inserts and one Sandvik R245 12T3 E-W CB50 wiper according to the Sandvik Coromant concept for bimetal machining.

3. Wear Mechanism

In general, during interrupted cutting operations, the tool is subjected to repeated thermal and mechanical fluctuating stresses. The main wear mechanisms in milling process are the mechanical fracture (chipping) as a result of repeated cutting force changes and the comb cracks due to alternating thermal stresses [3]. Therefore, the tool life in milling operation is largely influenced by the thermal and mechanical properties of the tool material, microgeometry of the inserts, the cutting conditions, the tool path, and in general, all the factors that control the stress level on inserts.

When milling aluminum-GCI engine blocks, the tool is engaged in cutting of two materials with extremely different mechanical properties; the soft and sticky aluminum alloy at elevated temperatures and the more high strength but brittle GCI as the liner material. In fact, the appropriate cutting conditions and tool material/geometry for machining of each material differs substantially. In order to avoid smearing on the tool edge, cutting fluid should always be utilized when machining aluminum alloys, while in the case of GCI, it is often recommended to use dry condition to prevent thermal shock. PCD and carbides are commonly used for machining of Al-Si alloys. However, an investigation by Ng et al. [4] showed that edge rounding in carbides while being in contact with hard silicon particles during machining is the dominant wear mechanism, which can adversely affect the surface integrity. PCD, on the other hand, is the first choice for machining of Al-Si alloys, since the alloy is not reactive with diamond and the PCD possess extremely high hardness compared to cemented carbides, and consequently less edge rounding due to silicon particles [4] [5].

Although the coated and uncoated carbides can be used for milling of GCI at low and moderate cutting speeds, CBN tools are increasingly being used in high speed face milling of pearlitic cast irons to improve the production efficiency [6]. However, application of CBN tools for machining of aluminum alloy is not reported in literature.

Fig 1 and Fig 2 show the worn CBN inserts used for machining of bimetallic engine blocks in wet condition. As can be seen, the main wear mechanism is the comb cracks due to fluctuating thermal and mechanical stresses. These cracks are often initiated at the hottest point on the rake face [3] and propagate perpendicular to the cutting edge, which finally leads to chipping of the edge. The aluminum built up layer can also be seen on the flank side, even in presence of cutting fluid. However, its formation was limited.

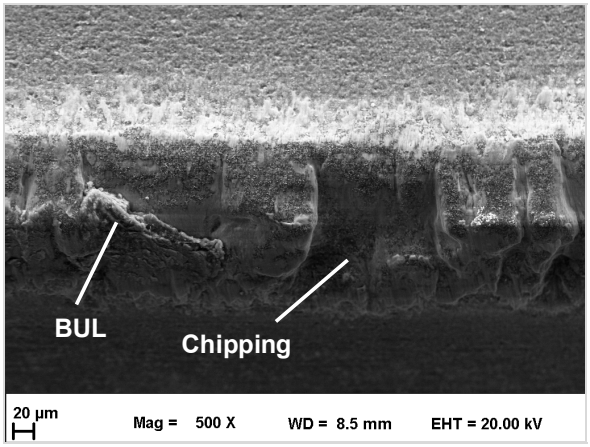

Fig. 1. The worn CBN insert. The formation of BUL on the flank face and chipping damage of the cutting edge

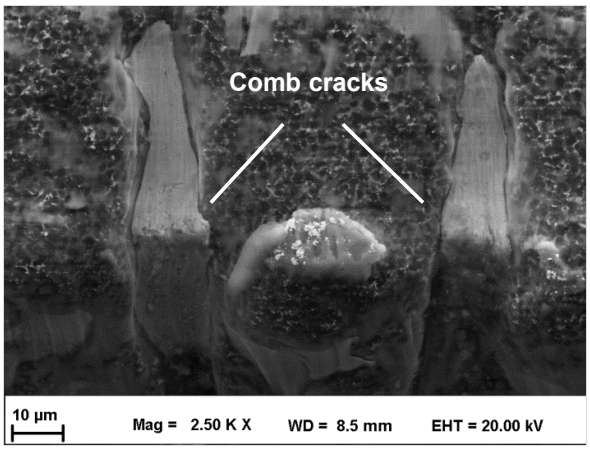

Fig. 2. The presence of thermal cracking at the cutting edge

4. Flow Stress Determination of Workpiece Material

In this study, flow stress properties of the aluminum alloy and GCI used in the engine block were determined by means of inverse methodology shown in Fig 3. In this method, first a series of orthogonal cutting tests at certain cutting conditions were carried out and the cutting/thrust forces, chip thickness (CT) and the tool/chip contact length (CL) on the inserts were measured accordingly. In the next stage, 2D FE models were built at the similar cutting conditions as the orthogonal cutting experiment. Using the concept of Response Surface Methodology (RSM) and Central Composite Design (CCD), different sets of material parameters for the Johnson-Cook (JC) constitutive

model were generated and provided as inputs for FE models. The results of FE simulations, including the forces, CT and CL, were provided for regression analysis to determine the 2nd order response surface relating the JC parameters to the output of interest. In the final stage, the response surfaces were compared with the respective experimental measurements and JC parameters were updated constantly to minimize the difference between the simulated and experimental results. Once the difference was smaller than an error tolerance, the optimal JC parameters were determined.

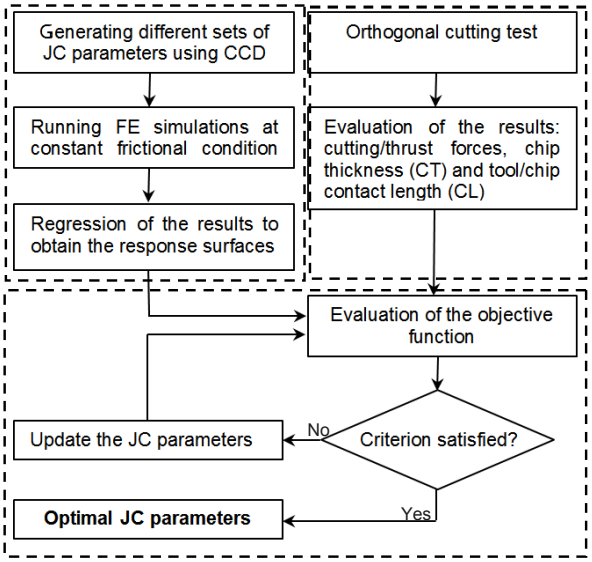

Fig. 3. Inverse methodology to determine the flow stress properties of workpiece material.

4.1. Experimental procedure

All the machining tests were carried out on a EMCO 365 CNC lathe, equipped with a Kistler Type 9257A three component dynamometer. Initially, several flanges were made with constant width of 2 mm for orthogonal cutting. For both aluminum alloy and GCI, the feed rate was kept constant at 0.1 mm/rev, while the cutting speed was varied in two levels. In all cases, N151.2-650-50-3B H13A cemented carbide inserts with a 0˚ rake angle and 10˚ clearing angle were used for orthogonal cutting tests in dry condition. Each test was repeated three times with fresh inserts to ensure the reproducibility of the measurements and the average cutting/thrust forces were provided for flow stress determination algorithm.

In order to measure the average chip thickness at different cutting conditions, three pieces from each repetition were randomly selected and mounted using the transparent thermoset. Care was taken to avoid inclination of the chips while mounting. A Zeiss optical microscope equipped with image processing software AxioVision was used to measure the chip thickness. The contact lengths were measured using elemental maps obtained from EDS (Energy Dispersive Spectroscopy) analysis on the rake face of each insert and the average values of three repetitions were recorded.

4.2. Response surface methodology and FE modeling of orthogonal cutting

In this study, DEFORM 2D commercial code was used to simulate the orthogonal cutting test as a part of inverse algorithm. A two dimensional FE model was built assuming a rigid tool and rigid-perfectly plastic workpiece material. However, heat transfer within the tool was allowed. JC constitutive model (see Equation 1) was used to simulate the plastic behavior of the workpiece material and the aim, here, was to determine the parameters of the constitutive model for the aluminum alloy and GCI.

$$\sigma = \left(A + B\varepsilon^{n}\right)\left[1 + C\ln\left(\frac{\dot{\varepsilon}}{\dot{\varepsilon}_0}\right)\right]\left[1 - \left(\frac{T - T_r}{T - T_m}\right)^{m}\right] \quad (1)$$

In Equation 1, σ is the flow stress of the material, ε is the strain, T is the temperature and $\dot{\varepsilon}$ is the strain rate, A, B, C, n and m are the material parameters, $\dot{\varepsilon}_0$ is the reference strain rate and T_m and T_r are melting and room temperatures, respectively.

Only 4mm segment was modeled to reduce the number of elements and consequently the solution time. The workpiece includes approximately 10000 elements. By means of mesh window technology, the mesh density close to the cutting edge and the rake face was controlled to maintain the element size constant at 5µm during the chip formation. The feed rate and the cutting speeds were set similar to the orthogonal cutting tests for each material. JMatPro™ software [7] was used to obtain temperature dependent thermal properties for the aluminum alloy, while the thermal properties for GCI were taken from [8]. The heat transfer coefficient between the tool and chip interface was assumed to be 10^5 N/s.mm.C to ensure that the heat transfer reaches steady state condition at the end of the simulations. A user subroutine was developed to include pressure dependent shear friction model at chip/tool interface using the equation:

$$\tau = m_0\left[1 - \exp(\alpha P)\right]k \quad (2)$$

where τ is the frictional shear stress, k is the shear strength of the workpiece material, P is the pressure and α and m_0 are the model constants. In all FE simulations, α is kept constant at 0.012 and 0.0035 for the aluminum alloy and GCI, respectively, and m_0=1.

In this work, central composite design was used to construct the second order response surfaces with the least number of combinations for JC material

parameters. It can be shown that using CCD algorithm; only 27 different combinations are required to construct the response surfaces for five variables in three levels. To this end, an initial guess for JC parameters was made for a certain material, and all different combinations were generated around the central point accordingly. Therefore, at each cutting condition, 27 FE simulations were performed providing the JC material parameters. The responses ($\mathbf{Y_m}$) including the forces, chip thickness and the contact length were then related to the JC parameters (x) in quadratic form as,

$$\mathbf{Y_m} = \beta_0 + \sum_{j=1}^{k} \beta_j x_j + \sum_{j=1}^{k} \beta_{jj} x_j^2 + \sum_i \sum_j \beta_{ij} x_i x_j \qquad (3)$$

where β represents the unknown coefficients determined by regression analysis for each response separately.

4.3. Optimization procedure

Determination of the JC parameters can be considered as an optimization problem, i.e. to minimize the objective function:

$$\mathrm{F}(\mathbf{X}) \quad x_L \leq \mathbf{X}_k \leq x_U \qquad (4)$$

where $\mathbf{X}$ is a vector including the JC parameters, x_L and x_U are the lower and upper bounds of each parameter and $\mathrm{F}(\mathbf{X})$ is the objective function expressed as:

$$\mathrm{F}(\mathbf{X}) = \sum_{m=1}^{4} \left\{ w_m \left[\sum_{n=1}^{N} \left(\frac{Y_{mn} - Y_{mn,EXP}}{Y_{mn,EXP}} \right)^2 \right] \right\} \qquad (5)$$

where w_m represents the weight factors and $Y_{mn,EXP}$ values are the respective experimental measurements at the same cutting condition as the response surface (Y_{mn}) generated by means of FEM and RSM as functions of JC parameters. The parameter N is the number of cutting conditions used for inverse determination of material parameters.

The JC parameters determined for both materials are given in Table 1. The comparison between 2D FE results incorporating the optimal JC parameters and the experimental measurements are shown in Fig 4 and Fig 5 for the aluminum alloy and GCI, respectively.

Table 1. JC material parameters for AlSi9Cu3Fe and GCI

Mat.	A(MPa)	B(MPa)	C	n	m	T_m(°C)
Al	250	157	0.024	0.158	0.9	495
GCI	470	250	0.004	0.1	1.1	1200

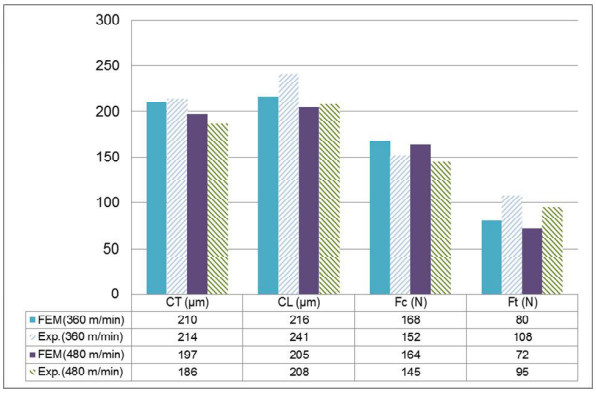

Fig. 4. The comparison between FE results and the experimental measurements for AlSi9Cu3Fe

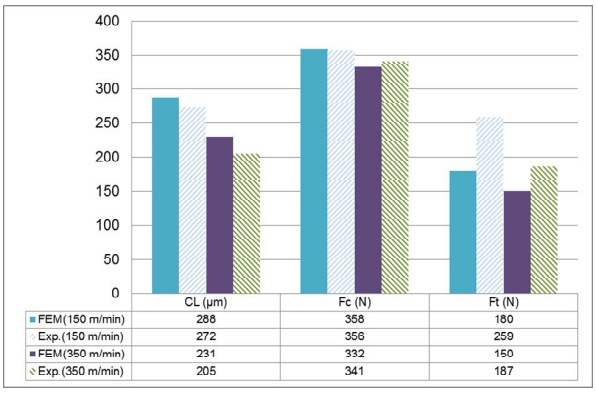

Fig. 5. The comparison between FE results and the experimental measurements for GCI

5. FE Modeling of 3D Milling

Simulation of different machining processes in 3D has been attempted by several researchers; however, they were mostly limited to turning process. Özel et al. [9] presented FE modeling of 3D turning process and investigated the effect of uniform and variable edge micro-geometry on the wear rates of PcBN inserts. Klocke and Krats [10] simulated the hard turning process and optimized the chamfer design to reduce the wear rate and improve the surface integrity. Pittala and Monno [11] utilized 3D approach to model face milling operation considering the real tool geometry for an aluminum alloy. Man et al. [12] utilized 3D FEM to simulate the milling process at different cutting conditions for Al7050-T7451 aluminum alloy and showed good correlation between predictions and experimental measurements.

In this study, 3D DEFORM^{TM} commercial code was used to simulate the milling operation. Only 5° of the cut was simulated to reduce the computational time. However, care was taken to ensure that the temperature on the rake face reaches steady state condition at the end of the run. The cutting process for aluminum alloy and

GCI were simulated separately. In order to avoid extremely large number of elements required for simulations of finishing operation, the tool was positioned at the maximum uncut chip thickness with respect to the workpiece with this thickness kept constant during 5˚ of cut. This simulation strategy results in extreme loading condition on the tool edge that can occur in one full rotation of the cutter. Decoupled tool stress analysis was performed to obtain thermal and mechanical stresses. In this method, initially, cutting process was simulated for each material with a rigid tool. However, heat transfer between the tool and workpiece was allowed during cutting process. Pressure dependent shear friction model given in Equation 2 with similar friction constants as used in 2D FE simulations were utilized here. Fig 6 shows the temperature distribution on the CBN inserts at the end of the cut for GCI and the aluminum alloy.

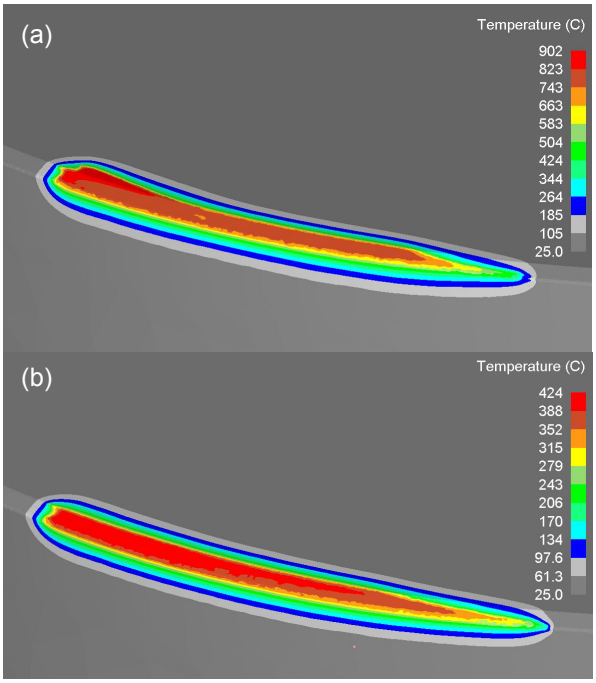

Fig. 6. Temperature distribution on the tool rake face after machining of (a) GCI and (b) aluminum alloy.

In a separate simulation, elastic properties for the tool were defined and nodal forces were extracted from the workpiece at the tool/chip interface and interpolated on the tool. The model ran under isothermal condition to obtain the mechanically induced stresses during cutting process. Fig 8 shows the stresses built up on the tool edge when machining of AlSi9Cu3Fe and GCI separately.

In order to simulate the thermally induced stresses as the tool leaves the workpiece, elasto-plastic formulation is used for the tool. A large value for the yield stress was assumed to avoid plastic deformation in the tool. The reason for using elasto-plastic formulation was to allow accumulation of dilatation strains due to thermal contraction at the end of each time step when cooling down to the room temperature. The results are shown in Fig 8 for GCI and the aluminum alloy.

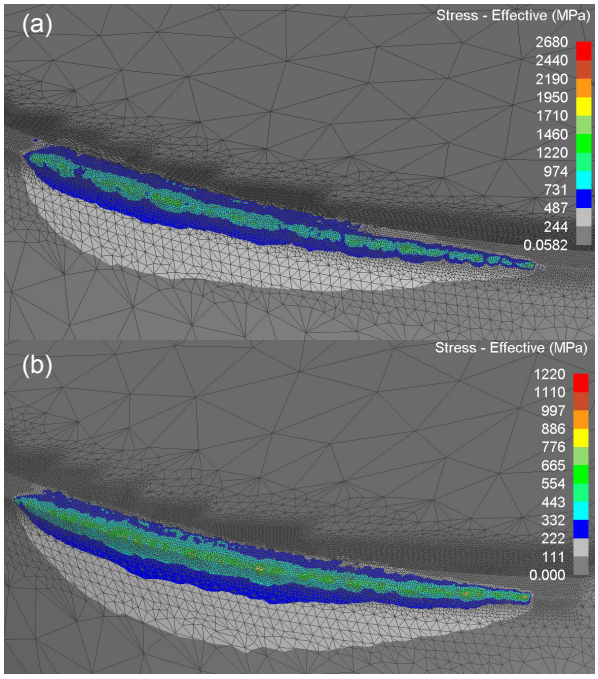

Fig. 7. Mechanically induced stresses during cutting process (a) GCI and (b) aluminum alloy.

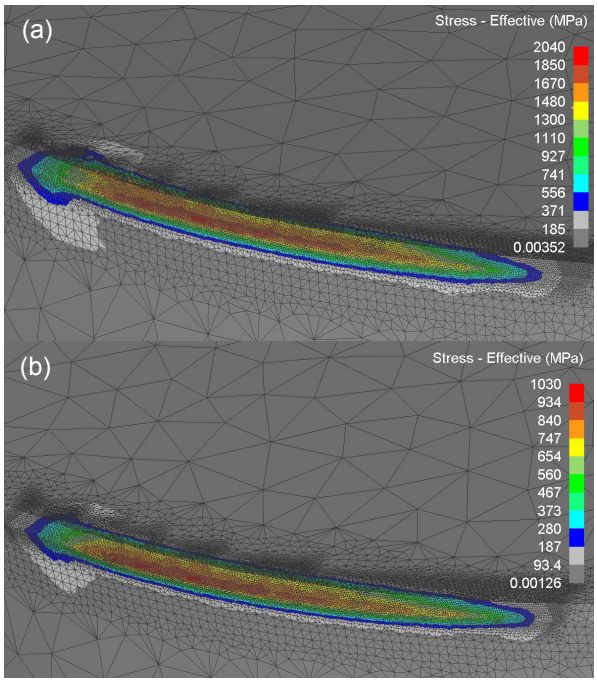

Fig. 8. Thermally induced stresses when cooling down to room temperature (a) GCI and (b) aluminum alloy.

Table 2 shows the built up von Mises stresses during cutting, and after cooling down to room temperature on two positions; one on the edge and the other on the rake face. In order to indicate the compressive or tensile nature of the stresses, the sign of mean stress was used. As can be seen, both thermal and mechanical stresses are higher when machining GCI. Hence, thermal cracking of the tool was at risk as also confirmed by the wear analysis.

Table 2. von Mises thermal and mechanical stresses

Material	Mechanical stress (MPa)		Thermal stress (MPa)	
	Rake	Edge	Rake	Edge
GCI	-753	-1550	1510	1910
Al	-470	-708	766	939

6. Conclusion

Wear mechanism of CBN inserts during face milling of bimetallic engine block was shown to include thermal cracking as the main wear mechanism. An inverse methodology was hence presented to determine the flow stress properties and the final implemented 3D FE simulation results showed that machining of GCI induces large thermal and mechanical stresses on the tool edge, although it only comprises less than 5% of machined area. The temperature when machining GCI is nearly two times higher than that for aluminum at the same cutting condition. The methodology presented in this study can be used to find the optimum cutting conditions and/or tool microgeometry in terms of low wear development and long tool life.

Acknowledgements

The authors acknowledge VINNOVA (Swedish Agency for Innovation Systems) within the framework of the FFI programme and the strategic initiative in production at Chalmers University of Technology for financial support. Special thanks are also extended to Lars Hellström and Leif Dhal from Sandvik Coromant and Dr. Peter Sotkovszki from Chalmers University of Technology for their support.

References

[1] Uthayakumar, M., Prabhakaran, G., Aravindan, S., Sivaprasad, J.,-V., 2012, Influence of Cutting Force on Bimetallic Piston Machining by a Cubic Boron Nitride (CBN) Tool, Materials and Manufacturing Processes,27:1078-1083.

[2] Correa, D.-C., Sales, W.-F., Santos, S.-C., Palma, E.-S., 2005, Machinability of Bimetallic Bearings Using Cemented Carbide Tools: Evaluation of the Wear Mechanisms, Journal of Materials Processing Technology 159: 435–444.

[3] Melo, A.C.-A, Milan, J.C.-G., Silva, M.-B., Machado, A.-R., 2006, Some Observations on Wear and Damages in Cemented Carbide Tools, Journal of the Brazilian Society of Mechanical Science and Engineering, 28/3:269-277.

[4] Ng, E.-G, Szablewski, D., Dumitrescu, M., Elbestawi, M.-A., Sokolowski, J.-H., 2004, High Speed Face Milling of a Aluminium Silicon Alloy Casting, CIRP Annals, 53/1:69-72.

[5] Lacalle, L.N.-L., Lamikiz, A., Sanchez, J.-A., Cabanes, I., 2001, Cutting Conditions and Tool Optimization in the High Speed Milling of Aluminium Alloys, Proceedings of the Institution of Mechanical Engineers, Part B: Journal of Engineering Manufacturing, 215:1257-1269.

[6] Liu, J., Yamazaki, K., Ueda, H., Narutaki, N., Yamane, Y., 2002, Machinability of Pearlitic Cast Iron with Cubic Boron Nitride (CBN) Cutting Tools, Transactions of ASME, 124:820-832.

[7] Guo, Z., Saunders, N., Miodownik, A.-P., Schillé, J.-Ph., 2009, Materials Properties for Process Simulation, Materials Science and Engineering A, 499:7-13.

[8] Data Handbook for Grey Irons, 1997, The Casting Development Center.

[9] Özel, T., Karpat, Y., Srivastava, A., 2008, Hard Turning with Variable Micro-geometry PcBN Tools, CIRP Annals, 57/1:73-76

[10] Klocke, F., Kratz, H., 2005, Advanced Tool Edge Geometry for High Precision Hard Turning, CIRP Annals, 53/1:47-50

[11] Pittala, G.-M., Monno, M., 2009, 3D Finite Element Modeling of Face Milling of Continuous Chip Material, International Journal of Advanced Manufacturing Technology, 47:543-555.

[12] Man, X., Ren, D., Usui, S., Johnson, C., Marusich T.-D., 2012, Validation of Finite Element Cutting Force Prediction for End Milling, Procedia CIRP, 1:692-697